JGP Journal of General Physiology

COMMUNICATION

Intracellular and extracellular loops of LRRC8 are essential for volume-regulated anion channel function

Toshiki Yamada and Kevin Strange

The volume-regulated anion channel (VRAC) is expressed ubiquitously in vertebrate cells and mediates swelling-induced release of Cl^- and organic solutes. Recent studies by several laboratories have demonstrated conclusively that VRAC is encoded by members of the leucine-rich repeat containing 8 (*Lrrc8*) gene family, which comprises five members, termed *Lrrc8a–e*. Numerous observations indicate that VRAC is a heteromeric channel comprising the essential subunit LRRC8A and one or more of the other LRRC8 paralogs. Here we demonstrate that the intracellular loop (IL) connecting transmembrane domains 2 and 3 of LRRC8A and the first extracellular loop (EL1) connecting transmembrane domains 1 and 2 of LRRC8C, LRRC8D, or LRRC8E are both essential for VRAC activity. We generate homomeric VRACs by replacing EL1 of LRRC8A with that of LRRC8C and demonstrate normal regulation by cell swelling and shrinkage. We also observe normal volume-dependent regulation in VRAC homomers in which the IL of LRRC8C, LRRC8D, or LRRC8E is replaced with the LRRC8A IL. A 25–amino acid sequence unique to the LRRC8A IL is sufficient to generate homomeric VRAC activity when inserted into the corresponding region of LRRC8C and LRRC8E. LRRC8 chimeras containing these partial LRRC8A IL sequences exhibit altered anion permeability, rectification, and voltage sensitivity, suggesting that the LRRC8A IL plays a role in VRAC pore structure and function. Our studies provide important new insights into the structure/function roles of the LRRC8 EL1 and IL. Homomeric LRRC8 channels will simplify future studies aimed at understanding channel structure and the longstanding and vexing problem of how VRAC is regulated by cell volume changes.

Introduction

Regulation of cell volume in response to intracellular and extracellular osmotic perturbations is an essential cellular physiological process (Hoffmann et al., 2009; Jentsch, 2016). In response to cell swelling, plasma membrane solute efflux mechanisms are activated to mediate regulatory volume decrease. The volume-regulated anion channel (VRAC) is expressed ubiquitously in vertebrate cells and mediates the swelling-induced release of Cl^- and organic solutes (Hoffmann et al., 2009; Jentsch, 2016).

The molecular identity of VRAC has been a source of significant controversy for two decades (Wine and Luckie, 1996; Strange, 1998; Nilius and Droogmans, 2003). However, two laboratories recently demonstrated that VRAC is encoded by members of the leucine-rich repeat containing 8 (*Lrrc8*) gene family (Qiu et al., 2014; Voss et al., 2014). These studies have subsequently been confirmed by several other groups (Hyzinski-García et al., 2014; Yamada et al., 2016; Gradogna et al., 2017).

The *Lrrc8* gene family comprises five members termed *Lrrc8a*, *Lrrc8b*, *Lrrc8c*, *Lrrc8d*, and *Lrrc8e* (Abascal and Zardoya, 2012; Voss et al., 2014). LRRC8A must be coexpressed with another family member to functionally reconstitute VRAC activity (Voss et al., 2014). VRACs observed in cells coexpressing LRRC8A + LRRC8C, LRRC8A + LRRC8D, or LRRC8A + LRRC8E exhibit unique permeability and voltage-dependent properties (Voss et al., 2014; Planells-Cases et al., 2015; Syeda et al., 2016; Ullrich et al., 2016; Lutter et al., 2017; Schober et al., 2017) and respond differently to reactive oxygen species (Gradogna et al., 2017). Immunoprecipitation (Voss et al., 2014; Syeda et al., 2016; Lutter et al., 2017) and TIRF microscopy (Gaitán-Peñas et al., 2016) studies suggest that LRRC8 proteins interact in vivo. Collectively, these findings indicate that VRAC is most likely a heteromeric channel formed by LRRC8A, an essential subunit, and LRRC8C, LRRC8D, and/or LRRC8E. The function of LRRC8B remains unclear and does not give rise to VRAC activity when

The MDI Biological Laboratory, Salisbury Cove, ME.

Correspondence to Kevin Strange: k.strange@mdibl.org.

heterologously coexpressed with LRRC8A (Voss et al., 2014; Gaitán-Peñas et al., 2016; Gradogna et al., 2017).

LRRC8 proteins contain four predicted transmembrane domains and a cytoplasmic C terminus with 15–17 predicted leucine-rich motifs that form a leucine-rich repeat (LRR) domain (Abascal and Zardoya, 2012; Fig. 1 A). The demonstration that LRRC8 proteins form heteromeric channels has important structure/function implications. Specifically, formation of a VRAC requires protein regions of LRRC8A and protein regions of one of the other LRRC8 paralogs. We demonstrate here that the intracellular loop (IL) connecting transmembrane domains 2 and 3 of LRRC8A and the first extracellular loop (EL1) connecting transmembrane domains 1 and 2 of LRRC8C, LRRC8D, or LRRC8E are both essential for VRAC activity. Homomeric VRACs with normal cell swelling- and shrinkage-induced regulation were generated by replacing EL1 of LRRC8A with that of LRRC8C. Normal volume-dependent regulation was also observed in VRAC homomers in which the IL of LRRC8C, LRRC8D, or LRRC8E was replaced with the LRRC8A IL. A 25–amino acid sequence unique to the LRRC8A IL was sufficient to generate homomeric VRAC activity when inserted into the corresponding region of LRRC8C and LRRC8E.

The electrophysiological properties of VRAC chimeric homomers were similar to those of VRAC heteromers. However, all chimeras exhibited differences in rectification, voltage-dependent inactivation, and/or anion permeability, suggesting that the IL of LRRC8A and EL1 of LRRC8C, LRRC8D, or LRRC8E may contribute to VRAC pore structure and function. Our results demonstrate that the LRRC8A IL and EL1 of LRRC8C, LRRC8D, or LRRC8E are essential for formation and function of VRACs and provide new insights into channel structure and regulation.

Materials and methods

Molecular biology

Human LRRC8A, LRRC8C, LRRC8D, and LRRC8E cDNAs cloned into pCMV6 were purchased from OriGene Technologies (catalog numbers RC226180, RC222603, RC203641, and RC209849, respectively). All cDNAs were tagged on their carboxy terminus with Myc-DDK epitopes. Mutant cDNA constructs were generated by using either the QuikChange Lightning Multi Site-Directed mutagenesis kits (Agilent Technologies) or the Phusion High-Fidelity PCR kit (New England BioLabs) and the restriction-free cloning method (Bond and Naus, 2012). Mutant and wild-type constructs were confirmed by DNA sequencing.

Transfection and whole-cell patch-clamp recording

Human colon cancer HCT116 cells in which the five *Lrrc8* genes were disrupted by genome editing (i.e., *Lrrc8*$^{-/-}$) were a gift from T. Jentsch. Cells were transfected by using Turbofectin 8.0 (OriGene Technologies) with 0.125 µg GFP cDNA and 0.15–1.0 µg of various LRRC8 cDNAs. All experimental protocols were performed on at least two independently transfected groups of cells.

Expression of heteromeric channels comprising the LRRC8A and LRRC8C paralogs was accomplished by transfecting cells with equal amounts of each cDNA. However, in our hands, we found it difficult to consistently detect VRAC activity in *Lrrc8*$^{-/-}$ cells cotransfected with equal amounts of LRRC8A and LRRC8D or LRRC8A and LRRC8E cDNAs. We have previously shown that reducing the amount of cotransfected LRRC8A cDNA by fivefold dramatically increases VRAC currents in *Lrrc8*$^{-/-}$ cells cotransfected with LRRC8C (Yamada et al., 2016). Therefore, LRRC8A + LRRC8D and LRRC8A + LRRC8E heteromeric channels were expressed by cotransfecting cells with 0.05 µg LRRC8A cDNA and 0.25 µg LRRC8D or LRRC8E cDNA.

Transfected cells were identified by GFP fluorescence and patch clamped by using a bath solution containing 75 mM CsCl, 5 mM $MgSO_4$, 2 mM calcium gluconate, 12 mM HEPES, 8 mM Tris, 5 mM glucose, 115 mM sucrose, and 2 mM glutamine, pH 7.4 (300 mOsm), and a pipette solution containing 126 mM CsCl, 2 mM $MgSO_4$, 20 mM HEPES, 6 mM CsOH, 1 mM EGTA, 2 mM ATP, 0.5 mM GTP, and 10 mM sucrose, pH 7.2 (275 mOsm). Cells were swollen and shrunken by exposure to 250 and 400 mOsm bath solutions, respectively. Osmolality was adjusted by addition or removal of sucrose. The total volume of the bath chamber used in these studies was ∼250 µl. Bath changes were performed by flushing the chamber for 1 min with at least 2 ml solution.

Patch electrodes were pulled from 1.5-mm–outer diameter silanized borosilicate microhematocrit tubes; electrode resistance ranged from 1 to 3 MΩ. Currents were measured with an Axopatch 200A (Axon Instruments) patch-clamp amplifier. Electrical connections to the patch-clamp amplifier were made by using Ag/AgCl wires and 3 M KCl/agar bridges. Series resistance was compensated by >85% to minimize voltage errors. Data acquisition and analysis were performed by using pClamp 10 software (Axon Instruments).

Quantification of LRRC8 current properties

Cells were dialyzed with pipette solutions for 2 min before current recordings were initiated. Membrane voltage was held at −30 mV, and whole-cell currents were elicited by voltage-ramping or -stepping protocols. For voltage ramps, membrane potential was first stepped to −100 mV and then ramped over 1 s to +100 mV. This was followed by a step back to −30 mV for 4 s before the ramp was repeated.

Step changes in membrane voltage were induced by first stepping membrane voltage to −80 mV for 0.5 s followed by steps from −120 mV to +120 mV in 2-s, 20-mV increments. Current–voltage relationships were generated by using the maximum current measured shortly after initiating the voltage step. Rectification ratios were estimated as the ratio of the maximum currents measured at +120 mV and −120 mV. Time constants for voltage-dependent channel inactivation were estimated by fitting a single exponential to currents elicited during a 2-s voltage step to +120 mV.

Anion permeability

Relative anion permeability (P_X/P_{Cl}) was measured from changes in reversal potential by using a modified Goldman–Hodgkin–Katz equation (Voss et al., 2014). Reversal potentials were corrected for anion-induced changes in liquid junction potentials. For these studies, the bath solution was switched from 75 mM NaCl to 75 mM NaI or 75 mM sodium gluconate.

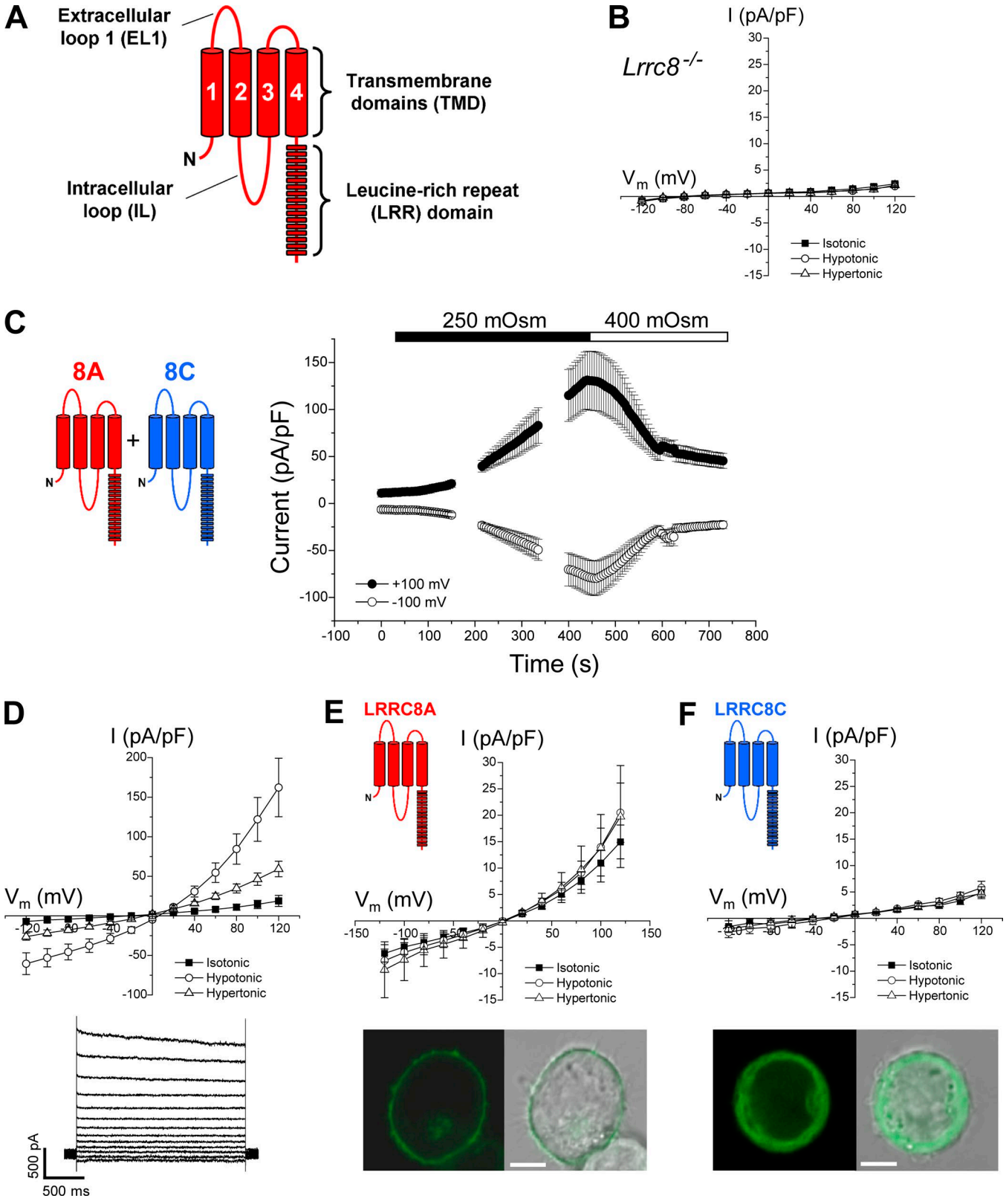

Figure 1. **Characteristics of LRRC8 channels. (A)** Cartoon showing key structural features of a LRRC8 protein. LRRC8 proteins comprise four predicted transmembrane domains (TMDs), a large EL1 connecting TMDs 1 and 2, an IL connecting TMDs 2 and 3, and a C-terminal LRR domain. **(B)** Current–voltage relationships of currents in *Lrrc8*$^{-/-}$ HCT116 cells transfected with GFP cDNA. Cell volume–sensitive anion currents are undetectable. Values are means ± SEM (n = 7). **(C)** Time course of swelling-induced activation and shrinkage-induced inactivation of whole-cell Cl^- currents in *Lrrc8*$^{-/-}$ HCT116 cells coexpressing LRRC8A and LRRC8C. Cells were swollen by exposure to a 250-mOsm bath solution and then shrunken by returning to hypertonic 400-mOsm bath. Values are means ± SEM (n = 7). **(D)** Current–voltage relationships (top) of basal current, peak swelling-induced current, and stable current observed after shrinking swollen cells in a hypertonic bath. Values are means ± SEM (n = 7). Representative traces (bottom) of swelling-activated 8A + 8C current. **(E)** Top: Current–voltage

Cell volume measurements

Cell volume was measured in all patch-clamp experiments to ensure (1) the absence of cell swelling or shrinkage induced by obtaining whole-cell access and (2) that volume changes were comparable between transfection and experimental protocols. Patch-clamped cells were visualized by video-enhanced differential interference contrast microscopy by using a Nikon TE300 microscope and Nikon Plan Fluor 60×/0.7 numerical aperture extra-long working distance lens. Images were captured by using a Dage-MTI CCD camera. The diameter of cells was measured at a single focal plane located at the point of maximum cell diameter. Cell morphology was assumed to approximate a sphere, and cell volume was calculated as $4/3 \times \pi \times r^3$, where r is the cell radius. Cells that exhibited volume changes in the absence of bath osmotic perturbations were not used for analysis of whole-cell current properties.

Confocal imaging

Distribution of GFP-tagged LRRC8 proteins was assessed by confocal imaging by using a Nikon TE2000-U microscope equipped with a Nikon C2+ confocal system and a Nikon S Fluor 40×/1.30 numerical aperture lens. Images were analyzed by using NIS-Elements C software.

Statistical analyses

Electrophysiological data are presented as means ± SEM; *n* represents the number of patch-clamped cells from which currents were recorded. Statistical significance was determined by using Student's *t* test for unpaired means.

Results

Fig. 1 A shows the predicted structural organization of LRRC8 proteins (Abascal and Zardoya, 2012). Swelling-activated anion currents were undetectable in *Lrrc8*$^{-/-}$ cells transfected with GFP alone (Fig. 1 B). In contrast, coexpression of LRRC8A (8A) and LRRC8C (8C) in *Lrrc8*$^{-/-}$ cells gave rise to a swelling-activated, outwardly rectifying anion current that was inactivated by cell shrinkage (Fig. 1 C). The mean reversal potential (Erev) of the swelling-activated current was 12.2 mV (Table 1), which is close to the expected Erev of 13 mV for a channel with high Cl^- over cation selectivity.

Expression of 8A alone gave rise to small outwardly rectifying currents that were insensitive to cell swelling or shrinkage (Fig. 1 E, top). GFP-tagged 8A appeared to be localized to the plasma membrane (Fig. 1 E, bottom). The Erev of the current under isotonic conditions was 2.9 ± 2.1 mV (n = 6), suggesting that the channel does not discriminate between Cl^- and Cs^+, which is the predominant intracellular and extracellular cation. This current may be caused by a nonselective channel formed by LRRC8A or it could be an unrelated current activated by expression of LRRC8A cDNA. No current above that seen in *Lrrc8*$^{-/-}$ cells (Fig. 1 B) was detected in cells expressing 8C alone (Fig. 1 F, top), and GFP-tagged 8C appeared to be present primarily in the cytoplasm (Fig. 1 F, bottom).

How anion channels that detect cell volume changes are formed from different LRRC8 proteins is unknown. LRRC8A is an essential subunit of VRAC and must be coexpressed with LRRC8C, LRRC8D, or LRRC8E to reconstitute normal volume-sensitive anion channel activity (Voss et al., 2014). LRRC8A appears to traffic to the cell membrane when expressed alone (Fig. 1 E; Voss et al., 2014). LRRC8C, LRRC8D, and LRRC8E expressed alone do not traffic to the cell membrane (Fig. 1 F; Voss et al., 2014). These findings demonstrate that correct assembly of VRAC requires one or more unique protein regions of LRRC8A and an additional protein region(s) from LRRC8C, LRRC8D, or LRRC8E. We used a chimera approach to create homomeric channels and identify LRRC8 protein regions required for normal VRAC function.

Sequence analysis demonstrated that two regions show striking sequence variation between LRRC8 paralogs. These regions are an IL of ∼120 amino acids connecting transmembrane domains 2 and 3 and an ∼80– to 124–amino acid EL1 connecting the first and second transmembrane domains (Figs. 1 A and 2).

Significant amino acid sequence variation between LRRC8 paralogs is observed in IL over a stretch of ∼60 amino acids roughly in the middle of the loop (Fig. 2, top). A chimera comprising 8A with the IL of 8C, 8A-8C(IL), did not give rise to measurable currents. In contrast, homomeric 8C-8A(IL) chimeras showed robust cell volume–dependent activity (Fig. 3).

Approximately 40–50% of cells expressing 8C-8A(IL) homomers appeared to be shrunken and could not be patch clamped. Of the 8C-8A(IL)–expressing cells from which recordings could be obtained, we observed two distinct populations. 57% (8 of 14 cells) of the cells patched, exhibited small resting currents that were stable upon obtaining whole cell access. These currents were strongly activated by cell swelling and inactivated by shrinkage (Fig. 3 A).

The second population of 8C-8A(IL)–expressing cells (43%; 6 of 14 cells) exhibited a current that activated slowly after whole-cell access was achieved (Fig. 3 B). Cell volume measurements demonstrated that this spontaneous activation occurred in the absence of detectable swelling. The relative cell volume measured 3 min after obtaining whole-cell access, which is when the current had stabilized (Fig. 3 B, left), was 1.0 ± 0.04 (n = 3). Spontaneously activated currents were inhibited by shrinking cells with a hypertonic bath solution and could be reactivated by cell swelling (Fig. 3 B). The magnitude of the peak swelling-induced current was two- to threefold larger than that of the spontaneously activated current (Fig. 3 B, left).

relationships of currents in LRRC8A-expressing cells. LRRC8A expression induces a small, outwardly rectifying current that is insensitive to cell volume changes. Values are means ± SEM (n = 5–6). Bottom: Fluorescent and brightfield images of a cell expressing LRRC8A with a C-terminal GFP tag. Bar, 5 µm. Protein appears to be localized primarily in or near the plasma membrane. **(F)** Top: Current–voltage relationships of currents in LRRC8C-expressing cells. Currents were not significantly different (P > 0.07) from those in GFP-expressing *Lrrc8*$^{-/-}$ HCT116 cells (see B). Values are means ± SEM (n = 7). Bottom: Fluorescent and brightfield images of a cell expressing LRRC8C with a C-terminal GFP tag. Bar, 5 µm. Protein appears to be localized primarily to the cytoplasm.

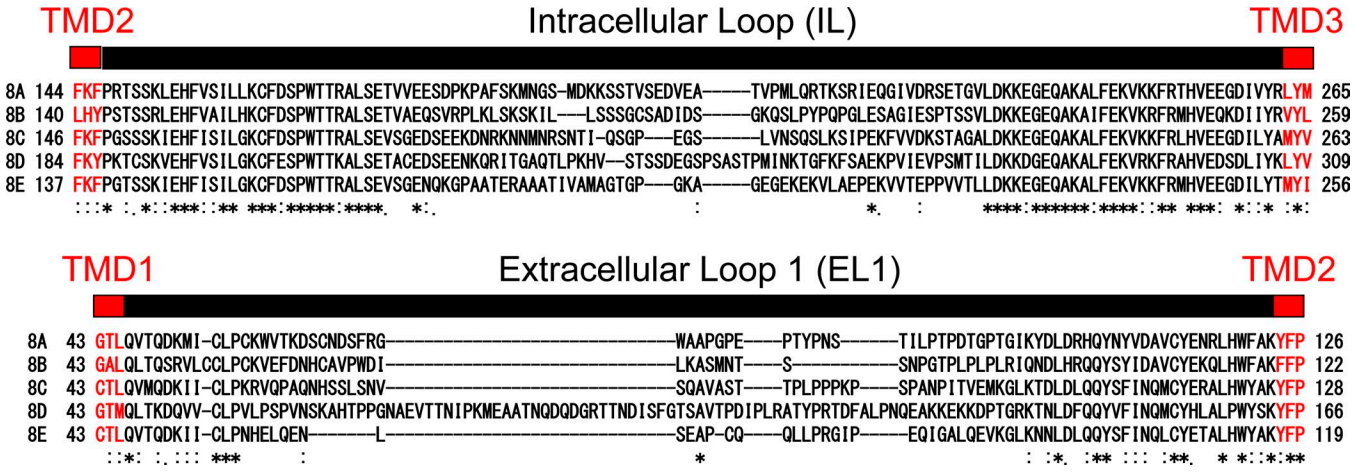

Figure 2. **Amino acid sequences and alignments of the EL1 connecting TMD1 and TMD2 and the IL connecting TMD2 and TMD3 of LRRC8A, LRRC8B, LRRC8C, LRRC8D. and LRRC8E.** TMD, transmembrane domain.

We also generated homomeric chimeras using LRRC8D (8D) and LRRC8E (8E). As with heteromeric 8A + 8D (Fig. 4 A) and 8A + 8E (Fig. 5 A) channels, homomeric 8D-8A(IL) (Fig. 4 B) and 8E-8A(IL) (Fig. 5 B) chimeras both generated robust VRAC currents that were activated by cell swelling and inactivated by cell shrinkage.

Electrophysiological properties of the VRAC LRRC8A IL chimeric homomers and VRAC heteromers are shown in Table 1. All chimeras were outwardly rectifying, exhibited reversal potentials close to the expected Cl^- Erev for an anion-selective channel, and had I^- and gluconate permeabilities greater and lesser than Cl^-, respectively. However, it is noteworthy that all the chimeras exhibited statistically significant differences in their electrophysiological properties when compared with heteromeric channels. For example, all chimeras had a significantly ($P < 0.0001$) higher relative I^- permeability compared with their respective heteromers (Table 1). 8C-8A(IL), 8D-8A(IL), and 8E-8A(IL) chimeras exhibited striking ($P < 0.0001$) changes in rectification (Table 1). Homomeric 8A-8C(EL1), 8D-8A(IL) and 8E-8A(IL) chimeras showed differences in voltage-dependent inactivation at +120 mV compared with heteromeric 8A + 8C, 8A + 8D, and 8A + 8E channels (Table 1).

To identify specific regions of the IL required for VRAC function, we created chimeras in which amino sequences of the LRRC8C IL were replaced with the corresponding sequence of the LRRC8A IL. Fig. 6 B shows peak swelling-activated currents observed in 8A + 8C heteromeric channels, the homomeric 8C-8A(IL) chimera engineered with the full length

Table 1. **Electrophysiological properties of swelling-activated anion conductances induced by expression of LRRC8 constructs in *LRRC8*$^{-/-}$ HCT116 cells**

Construct	Erev	Rectification	Inactivation at +120 mV	τ (ms) at +120 mV	PI/PCl	PGluc/PCl
	mV	$I_{+120\ mV}/I_{-120\ mV}$	I_{2s}/I_{max}			
8A + 8C	12.2 ± 0.3 (14)	2.65 ± 0.14 (7)	0.70 ± 0.03 (7)	3,268 ± 684 (7)	1.5 ± 0.02 (4)	0.19 ± 0.01 (3)
8A-8C(EL1)	10.6 ± 0.3 (9)	2.95 ± 0.21 (5)	1.01 ± 0.02 (5)	3,326 ± 1,298 (5)	2.1 ± 0.06 (4)	0.17 ± 0.02 (4)
	P < 0.002		P < 0.0001		P < 0.0001	
8C-8A(IL)	11.5 ± 0.3 (8)	1.86 ± 0.18 (6)	0.77 ± 0.06 (6)	2,507 ± 459 (6)	2.2 ± 0.04 (4)	0.26 ± 0.02 (4)
		P < 0.004			P < 0.0001	
8A + 8D	12.6 ± 0.5 (7)	5.35 ± 0.38 (7)	0.60 ± 0.04 (7)	2,206 ± 506 (7)	1.4 ± 0.03 (5)	0.26 ± 0.11 (5)
8D-8A(IL)	9.3 ± 0.2 (10)	1.98 ± 0.16 (5)	0.74 ± 0.03 (5)	1,917 ± 459 (5)	1.9 ± 0.03 (5)	0.28 ± 0.02 (4)
	P < 0.0005	P < 0.0001	P < 0.03		P < 0.0001	
8A + 8E	13.7 ± 0.4 (7)	2.52 ± 0.13 (6)	0.23 ± 0.05 (6)	947 ± 242 (6)	1.45 ± 0.02 (4)	0.20 ± 0.01 (4)
8E-8A(IL)	13.6 ± 0.4 (12)	5.28 ± 0.20 (6)	0.09 ± 0.01 (6)	181 ± 47 (6)	1.8 ± 0.02 (6)	0.12 ± 0.003 (5)
		P < 0.0001	P < 0.04	P < 0.01	P < 0.0001	P < 0.0001

Values are means ± SEM (*n*). Rectification was estimated as the ratio of peak currents (pA/pF) measured at +120 mV and −120 mV. P values are from comparison of a chimera to the relevant heteromer (e.g., 8A-8C[EL1] and 8C-8A[IL] compared with 8A + 8C).

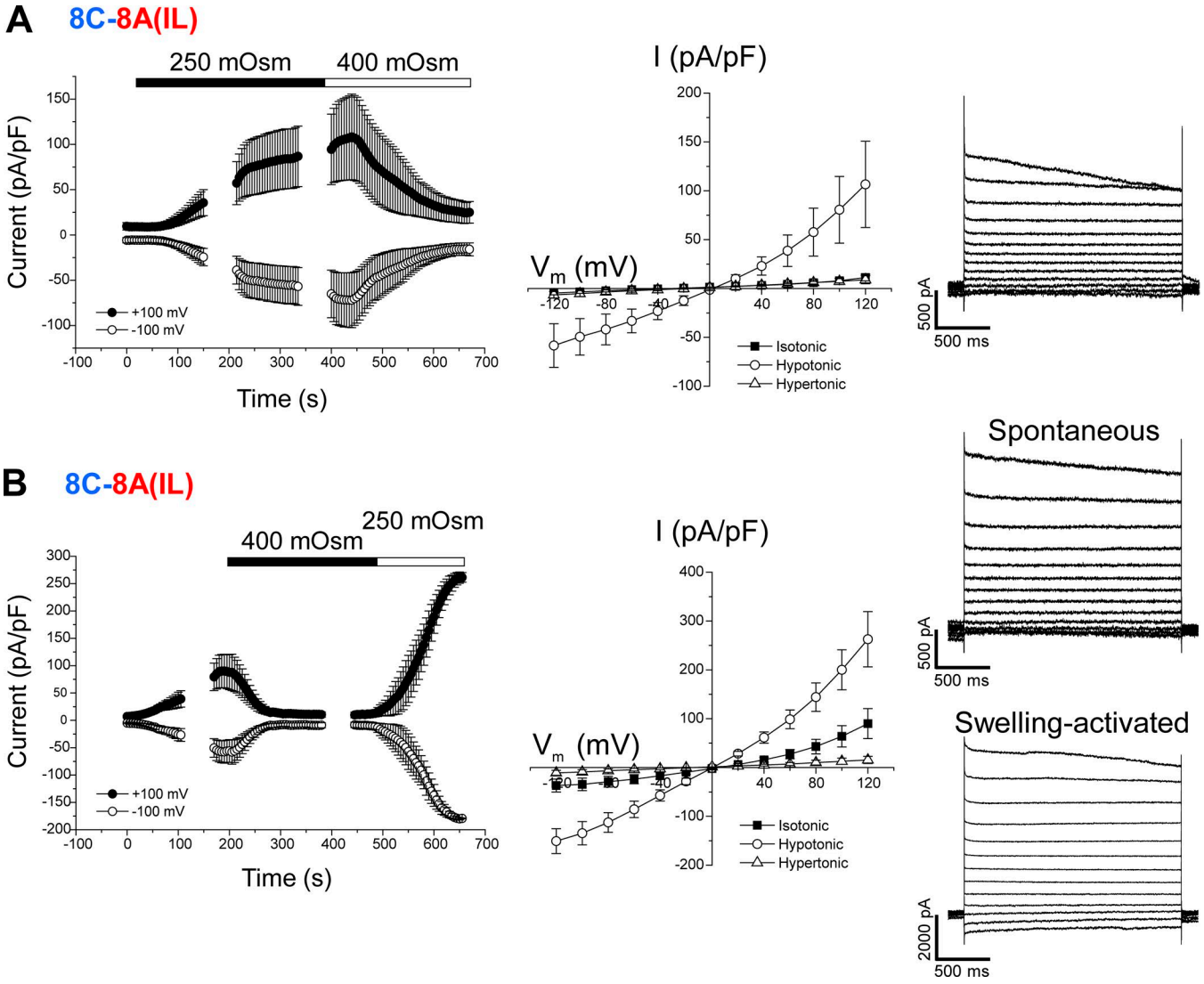

Figure 3. **Cell volume-sensitive currents induced by the homomeric 8C-8A(IL) chimera. (A)** Properties of VRAC currents observed in *Lrrc8*$^{-/-}$ 8C-8A(IL)-expressing HCT116 cells with stable resting currents. Left and middle panels show time course and current–voltage relationships of resting, swelling-activated, and shrinkage-inactivated currents. Values are means ± SEM (n = 4–5). Right panel shows representative traces of swelling-activated currents induced by the 8C-8A(IL) chimera. **(B)** Properties of spontaneously activating currents in *Lrrc8*$^{-/-}$ HCT116 cells expressing the 8C-8A(IL) chimera. Left panel shows time course of shrinkage-induced inactivation of the spontaneously activated current and reactivation by cell swelling. Middle panel shows current–voltage relationships of currents observed under isotonic conditions after cell shrinkage and reactivation by cell swelling. Values are means ± SEM (n = 3). Representative traces (right panel) of spontaneous and swelling-activated 8C-8A(IL) chimera-induced current observed in the same cell.

(P147–R262) 8A IL, and homomeric chimeras containing partial 8A IL sequence (Fig. 6 A). Swelling-activated currents with peak magnitudes similar to those of 8A + 8C heteromeric and 8C-8A(P147-R262) homomeric chimera channels were observed with the 8C-8A(P147–E206), 8C-8A(D182–E206), and 8C-8A(D182–V231) chimeras (Fig. 6 B). 8C-8A(P147–S181), 8C-8A(D182–N191), and 8C-8A(G192–E206) chimeras induced considerably smaller swelling-activated currents (Fig. 6 B). All chimeras that were activated by cell swelling were also inactivated by cell shrinkage (Fig. 6 C, top and data not depicted). 8C-8A(A207–V231) and 8C-8A(A207–R262) chimeras did not give rise to measurable currents. GFP-tagged constructs demonstrated that these chimeras were not trafficked to the cell membrane (unpublished data).

Analysis of the 8A IL sequence (Fig. 6 A) demonstrated that the three partial sequence chimeras that gave rise to robust swelling-activated currents contained amino acids D182–E206 (i.e., DPKPAFSKMNGSMDKKSSTVSEDVE). Fig. 6 C shows the time course of volume-sensitive current activation and inactivation; current–voltage relationships of resting, swelling-activated, and shrinkage-inactivated currents; and representative swelling-activated current traces induced by the 8C-8A(D182–E206) chimera.

For the 8C-8A(D182–E206) chimera, amino acids E184–E204 of the 8C IL were deleted and replaced with D182–E206 of the 8A IL. We also deleted E222–S248 of the 8D IL and K175–K197 of the 8E IL and replaced them with 8A IL D182–E206. The 8E-8A(D182–E206) chimera also gave rise to robust volume-sensitive currents (Fig. 6 D) that were similar to those observed in cells expressing

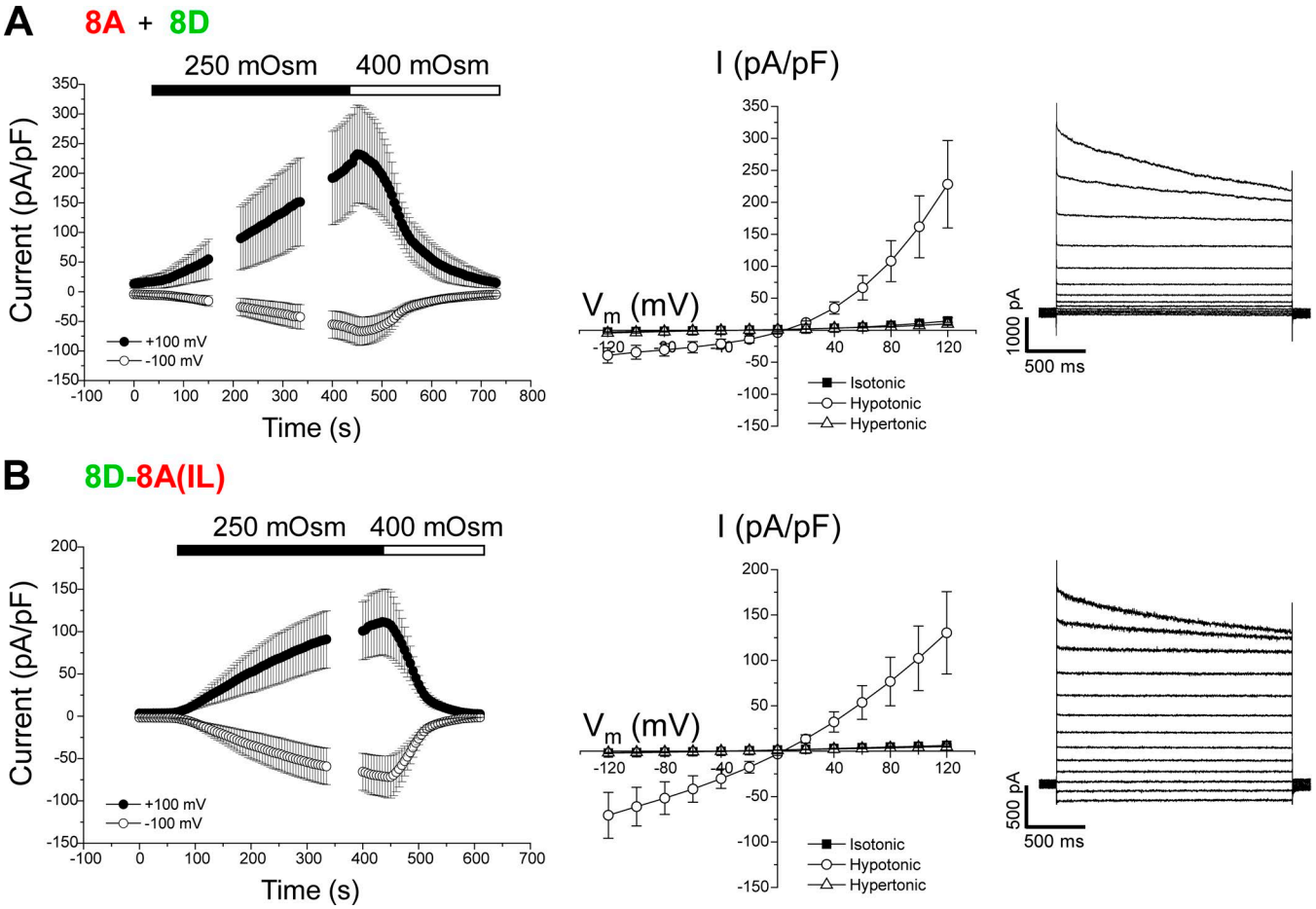

Figure 4. **Cell volume-sensitive currents induced by 8A + 8D heteromers and the homomeric 8D-8A(IL) chimera. (A)** Time course (left) and current–voltage relationships (middle) of resting, swelling-activated, and shrinkage-inactivated currents in *Lrrc8*$^{-/-}$ HCT116 cells coexpressing LRRC8A and LRRC8D. Values are means ± SEM (n = 4). Right panel shows representative traces of swelling-activated currents induced by 8A + 8D heteromers. **(B)** Time course (left) and current–voltage relationships (middle) of resting, swelling-activated, and shrinkage-inactivated currents in *Lrrc8*$^{-/-}$ HCT116 cells expressing the 8D-8A(IL) chimera. Values are means ± SEM (n = 4–5). Right panel shows representative traces of swelling-activated currents induced by 8D-8A(IL) homomers.

8A + 8E heteromers (Fig. 5 A). The 8D-8A(D182–E206) chimera did not give rise to anion current activity.

Table 2 shows the electrophysiological properties of the full-length and partial-sequence 8C-8A(IL) and 8E-8A(IL) chimeras. Interestingly, many of the partial-sequence chimeras had significantly altered electrophysiological properties. For example, the 8C-8A(D182–N191) chimera exhibited a significant reduction in Erev, suggesting a reduction in anion-over-cation selectivity. 8C-8A(P147–S181), 8C-8A(D182–E206), 8C-8A(G192–E206), and 8C-8A(D182–V231) chimeras all exhibited greatly increased voltage-dependent inactivation. The 8C-8A(D182–V231) chimera had reduced rectification.

Data in Figs. 3, 4, 5, and 6 demonstrate clearly that the IL of the essential VRAC subunit LRRC8A must be coexpressed with one or more protein regions of LRRC8C, LRRC8D, or LRRC8E to form a VRAC with normal volume-dependent regulation. As shown in Fig. 2 (bottom), EL1 is the other LRRC8 protein region that varies considerably between paralogs. To test whether EL1 must be coexpressed with the LRRC8A IL to form a VRAC, we substituted the LRRC8A EL1 with the EL1 from LRRC8C, LRRC8D, or LRRC8E. As shown in Fig. 7 A, the homomeric 8A-8C(EL1) chimera gave rise to stable resting currents that were strongly activated by cell swelling and inactivated by shrinkage.

An 8A-8D(EL1) chimera did not generate measurable currents (n = 10 cells). The homomeric 8A-8E(EL1) chimera gave rise to a small (current amplitude at +100 mV = 17.4 ± 3.5 pA/pF; n = 4) constitutively active outwardly rectifying current with an Erev of 8.0 ± 1.3 mV (n = 4), suggesting that the channel was selective for Cl^- over Cs^+. This current was insensitive to cell swelling but was fully inactivated by cell shrinkage (unpublished data).

Finally, we engineered 8A-8C(EL1) chimeras containing partial sequences of the 8C EL1 (Fig. 2, bottom) to identify regions critical for VRAC function. 8A-8C(Q46–K85), 8A-8C(K57–K97), and 8A-8C(K57–A119) chimeras did not give rise to measurable currents. Cells transfected with 0.25 µg 8A-8C(P86–K125) cDNA were severely shrunken and could not be patch clamped. Reducing the amount of transfected cDNA to 0.15 µg reduced cell shrinkage. Cells transfected with 0.15 µg 8A-8C(P86–K125) cDNA exhibited large, constitutively active, outwardly rectifying anion currents (Fig. 7 B). Erev for the constitutively active current was 12.3 ± 1.3 mV (n = 5), indicating that the 8A-8C(P86–K125) channel was anion selective. Interestingly, the 8A-8C(P86–K125)

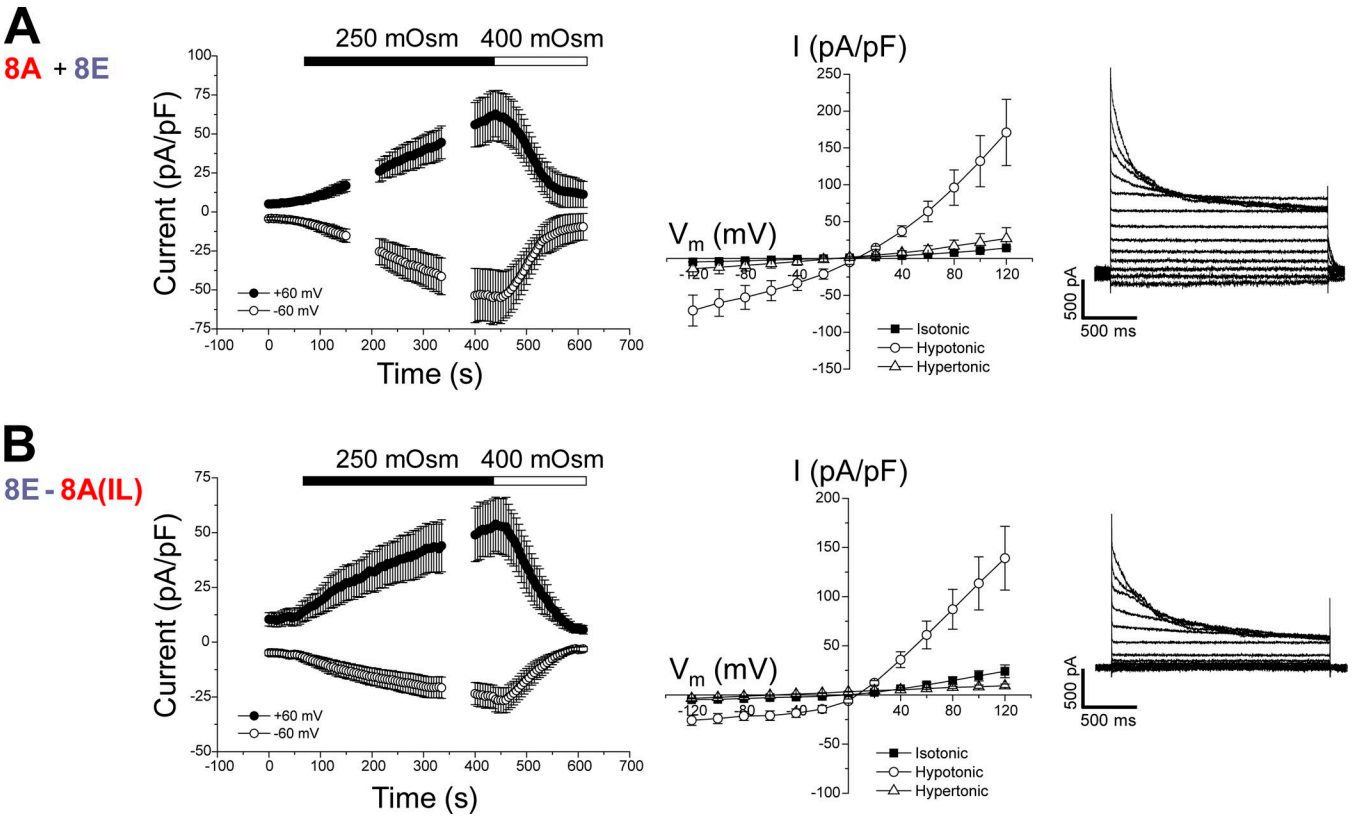

Figure 5. **Cell volume-sensitive currents induced by 8A + 8E heteromers and the homomeric 8E-8A(IL) chimera. (A)** Time course (left) and current–voltage relationships (middle) of resting, swelling-activated and shrinkage-inactivated currents in *Lrrc8*$^{-/-}$ HCT116 cells coexpressing LRRC8A and LRRC8E. Values are means ± SEM (n = 3). Right panel shows representative traces of swelling-activated currents induced by 8A + 8E heteromers. **(B)** Time course (left) and current–voltage relationships (middle) of resting, swelling-activated and shrinkage-inactivated currents in *Lrrc8*$^{-/-}$ HCT116 cells expressing the 8E-8A(IL) chimera. Values are means ± SEM (n = 4–6). Right panel shows representative traces of swelling-activated currents induced by 8E-8A(IL) homomers.

currents were strongly inactivated by cell shrinkage but insensitive to cell swelling (Fig. 7 B).

Discussion

VRACs are expressed ubiquitously in vertebrate cells and mediate the swelling-induced efflux of Cl^- and small organic solutes termed organic osmolytes (Hoffmann et al., 2009; Jentsch, 2016). It is now well-established that LRRC8 proteins are essential components of VRAC (Hyzinski-García et al., 2014; Qiu et al., 2014; Voss et al., 2014; Yamada et al., 2016; Gradogna et al., 2017). LRRC8 proteins are homologous to pannexins/innexins and appear to have diverged from this gene family at the origin of the chordates (Abascal and Zardoya, 2012). Pannexins function as nonselective membrane channels that mediate the passive flux of ions and small molecules such as ATP (Chiu et al., 2018). Innexins function as gap junction channels in invertebrates (Phelan, 2005).

Although they do not share sequence homology, LRRC8 proteins and pannexins/innexins are thought to have a membrane topology similar to that of connexins, which form vertebrate gap junctions, and calcium homeostasis modulator channels (Abascal and Zardoya, 2012; Ma et al., 2016; Chiu et al., 2018). All these channel types are capable of transporting small organic solutes and are thought to be formed by six subunits. However, only the structure of connexins, which form hexameric gap junction hemichannels, has been well-defined (Maeda et al., 2009). A recent cryo-EM study suggests that innexin-6 hemichannels have an octameric structure (Oshima et al., 2016). Biochemical data suggest that the structure of the pannexin2 channel may also be octameric (Ambrosi et al., 2010). No structural data exist for LRRC8 proteins and calcium homeostasis modulator.

All existing data indicate that VRACs are heteromers composed of the essential subunit LRRC8A and one or more of the other LRRC8 paralogs (Voss et al., 2014; Planells-Cases et al., 2015; Gaitán-Peñas et al., 2016; Syeda et al., 2016; Ullrich et al., 2016; Gradogna et al., 2017; Lutter et al., 2017; Schober et al., 2017). The stoichiometries and arrangement of subunits are unknown. We have demonstrated here that homomeric VRACs are formed from LRRC8 chimeras containing the LRRC8A IL and EL1 from LRRC8C, LRRC8D, or LRRC8E. 8A-8C(EL1), 8C-8A(IL), 8D-8A(IL), and 8E-8A(IL) chimeras all gave rise to robust volume-sensitive anion currents that were comparable to 8A + 8C, 8A + 8D, and 8A + 8E heteromers (Figs. 3, 4, 5, 6, and 7). The simplest interpretation of these results is that the LRRC8A IL and EL1 from LRRC8C, LRRC8D, or LRRC8E must be coexpressed in the same protein or in a heteromeric protein complex to form a VRAC.

The 8A-8D(EL1) and 8A-8E(EL1) chimeras did not give rise to normal VRAC activity. The reason why these chimeras were nonfunctional is unclear. It is possible that 8A-8D(EL1) and 8A-8E(EL1) chimeras require other structural components of LRRC8D and

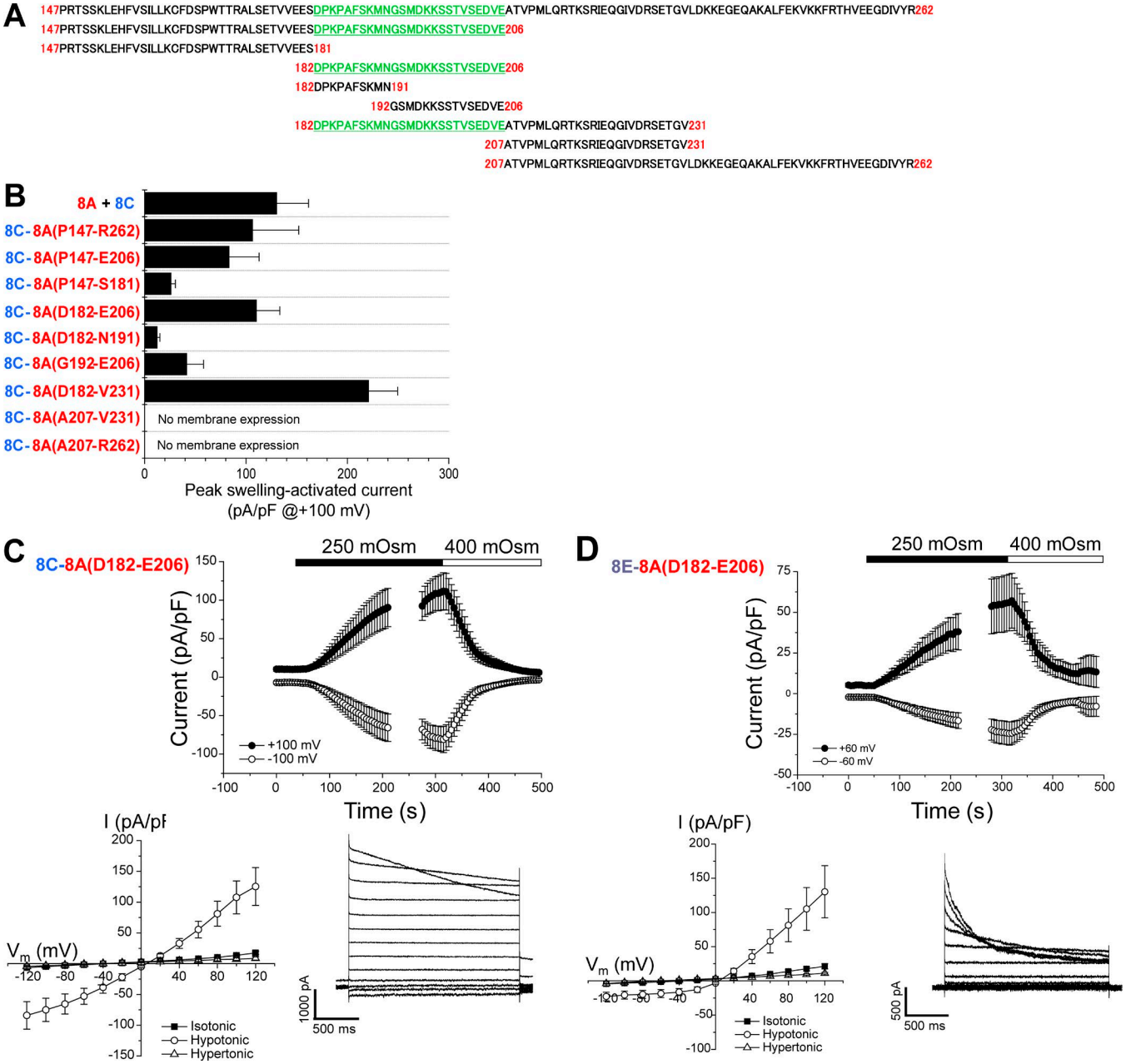

Figure 6. **Functional properties of chimeras containing partial sequence of the LRRC8A IL. (A)** Sequences of LRRC8A IL used for constructing 8C-8A(IL) chimeras. Amino acids P147–R262 represents the full-length LRRC8A IL. Region highlighted in green and underlined gave rise to peak swelling-activated currents similar to those observed in cells expressing 8A+8C heteromers. **(B)** Peak swelling-activated currents observed in various 8C-8A(IL) chimeras. No current was observed in 8C-8A(A207–V231) and 8C-8A(A207–R262) chimeras. GFP-tagged chimeras indicated that these chimeras were likely not expressed in the plasma membrane. Values are means ± SEM (n = 4–7). **(C)** Time course (top) and current–voltage relationships (bottom left) of resting, swelling-activated, and shrinkage-inactivated currents in *Lrrc8*$^{-/-}$ HCT116 cells expressing the 8C-8A(D182–E206) chimera. Values are means ± SEM (n = 7). Bottom right panel shows representative traces of swelling-activated currents induced by the 8C-8A(D182–E206) homomer. **(D)** Time course (top) and current–voltage relationships (bottom left) of resting, swelling-activated, and shrinkage-inactivated currents in *Lrrc8*$^{-/-}$ HCT116 cells expressing the 8E-8A(D182–E206) chimera. Values are means ± SEM (n = 5). Bottom right panel shows representative traces of swelling-activated currents induced by the 8E-8A(D182–E206) homomer.

LRRC8E to form a functional VRAC. It is also possible that transplanting EL1 of LRRC8D or LRRC8E into LRRC8A disrupts the translation, folding, and/or processing of the chimeric protein.

LRRC8C (Fig. 1 F), LRRC8D, and LRRC8E (Voss et al., 2014) do not traffic to the membrane when expressed alone. In contrast, LRRC8A expressed alone traffics to the cell membrane (Voss et al., 2014; Fig. 1 E) and may form an outwardly rectifying and apparently nonselective channel (Fig. 1 E). At a minimum then, it appears that the LRRC8A IL and EL1 of another LRRC8 protein are required for the assembly and/or trafficking of normal VRAC heteromers. As discussed below, these protein regions may also play important roles in VRAC pore structure and gating.

8C-8A chimeras containing partial sequences of the LRRC8A IL revealed important features of this protein region. Chimeras

Table 2. **Electrophysiological properties of swelling-activated anion conductances induced by expression of 8C-8A(IL) homomeric chimeras in *LRRC8*$^{-/-}$ HCT116 cells**

Construct	Erev	Rectification	Inactivation at +120 mV	τ (ms) at +120 mV
	mV	$I_{+120\ mV}/I_{-120\ mV}$	I_{2s}/I_{max}	
8C-8A(IL)	11.5 ± 0.3 (8)	1.86 ± 0.18 (6)	0.77 ± 0.06 (6)	2,507 ± 459 (6)
8C-8A(P147–E206)	11.7 ± 0.2 (6)	1.94 ± 0.15 (6)	0.61 ± 0.06 (6)	4,439 ± 870 (5)
8C-8A(P147–S181)	11.6 ± 0.5 (5)	1.71 ± 0.13 (5)	0.35 ± 0.11 (5)	2,878 ± 1473 (5)
			P < 0.04	
8C-8A(D182–E206)	11.5 ± 0.4 (7)	1.67 ± 0.21 (7)	0.37 ± 0.05 (7)	2,748 ± 685 (6)
			P < 0.003	
8C-8A(D182–N191)	8.5 ± 0.8 (5)	1.94 ± 0.22 (5)	0.46 ± 0.09 (5)	1,771 ± 372 (4)
	P < 0.002		P = 0.07	
8C-8A(G192–E206)	11.2 ± 0.4 (6)	2.24 ± 0.40 (6)	0.41 ± 0.06 (6)	4,118 ± 1,324 (6)
			P < 0.01	
8C-8A(D182–V231)	11.0 ± 0.3 (5)	1.23 ± 0.05 (5)	0.34 ± 0.04 (5)	2,224 ± 975 (5)
		P < 0.0001	P < 0.002	
8E-8A(IL)	13.6 ± 0.4 (12)	5.28 ± 0.20 (6)	0.09 ± 0.01 (6)	181 ± 47 (6)
8E-8A(D182–E206)	10.8 ± 0.6 (5)	5.68 ± 0.26 (5)	0.10 ± 0.01 (5)	333 ± 52 (5)
	P < 0.0001			

Values are means ± SEM (*n*). Rectification was estimated as the ratio of peak currents (pA/pF) measured at +120 mV and −120 mV. P values reflect comparisons of the 8C-8A(IL) or 8E-8A(IL) chimeras engineered with the full-length LRRC8A IL with chimeras engineered with partial LRRC8A IL amino sequences.

containing the C-terminal half (A207–R262) of the LRRC8A IL were not expressed in the cell membrane (Fig. 6, A and B). However, chimeras containing even small stretches of the N-terminal half of IL gave rise to anion-selective channels (Table 2) that were activated by cell swelling (Fig. 6 B) and inactivated by shrinkage (Fig. 6 C, top and unpublished data). All chimeras that gave rise to swelling-activated currents with peak magnitudes similar to that of 8A + 8C heteromers contained the D182–E206 sequence (Fig. 6). The 8E-8A(D182–E206) chimera (Fig. 6 D) also gave rise to VRAC activity similar to that observed with 8A + 8E heteromers (Fig. 5 A). Smaller swelling-activated currents were also observed in chimeras containing only part of the D182–E206 sequence (i.e., 8C-8A[D182–N191] and 8C-8A[G192–E206]) or lacking it altogether (i.e., 8C-8A[P147–S181]). It is unclear whether these chimeras exhibit lower membrane expression levels, have altered conductance, and/or have reduced responsiveness to cell swelling. We conclude that D182–E206 is the minimal sequence of the LRRC8A IL required for normal VRAC activity.

Sequence comparison shows remarkably high evolutionary conservation of the LRRC8A IL compared with ILs and EL1s of other LRRC8 paralogs. For example, cartilaginous fish such as the elephant shark and bony vertebrates diverged ∼450 million years ago. The genome of the elephant shark is the least derived among known vertebrates (Venkatesh et al., 2014). Basic Local Alignment Search Tool analysis of elephant shark and human LRRC8A ILs demonstrates that they share 93% identity, which implies an essential and highly conserved function of this LRRC8 protein region.

In silico secondary structure analyses with the use of JPred, RaptorX, and s2D programs predicted that the conserved regions of the ILs of LRRC8A, LRRC8C, LRRC8D, and LRRC8E (Fig. 2) contain helical structure. The region that shows substantial sequence variation among the four ILs is predicted to be random coil.

Predictor of Natural Disordered Regions (PONDR) VLXT analysis revealed interesting differences between the IL of LRRC8A and the ILs of LRRC8C, LRRC8D, and LRRC8E. Fig. 8 shows PONDR scores for the LRRC8A and LRRC8C ILs. A particularly interesting feature of the PONDR analysis is seen in the regions of the ILs lacking sequence homology. This region is predicted to be intrinsically disordered for the LRRC8C IL (Fig. 8) as well as the ILs of LRRC8D and LRRC8E (unpublished data). In contrast, the PONDR score for the LRRC8A IL takes a sharp dip in the region of the amino sequence we identified as the minimal sequence (i.e., D182–E206; Fig. 8) required to give rise to homomeric 8C-8A(D182–E206) and 8E-8A(D182–E206) VRACs with normal swelling-induced activity (Fig. 6, C and D). Such dips in the PONDR score of intrinsically disordered protein regions are thought to predict the existence of molecular recognition elements (MoREs) or features (MoRFs; Oldfield et al., 2005; Mohan et al., 2006; Xue et al., 2010). MoREs/MoRFs are small stretches of amino acid sequence within intrinsically disordered proteins regions that mediate protein–protein interactions.

The ILs of pannexins and connexins play important roles in channel function. For example, the ILs of various connexin subfamilies interact with and mediate the inhibitory effects of calmodulin on gap junctions (Zou et al., 2014). The IL of pannexin1 mediates a functional regulatory interaction with the α1

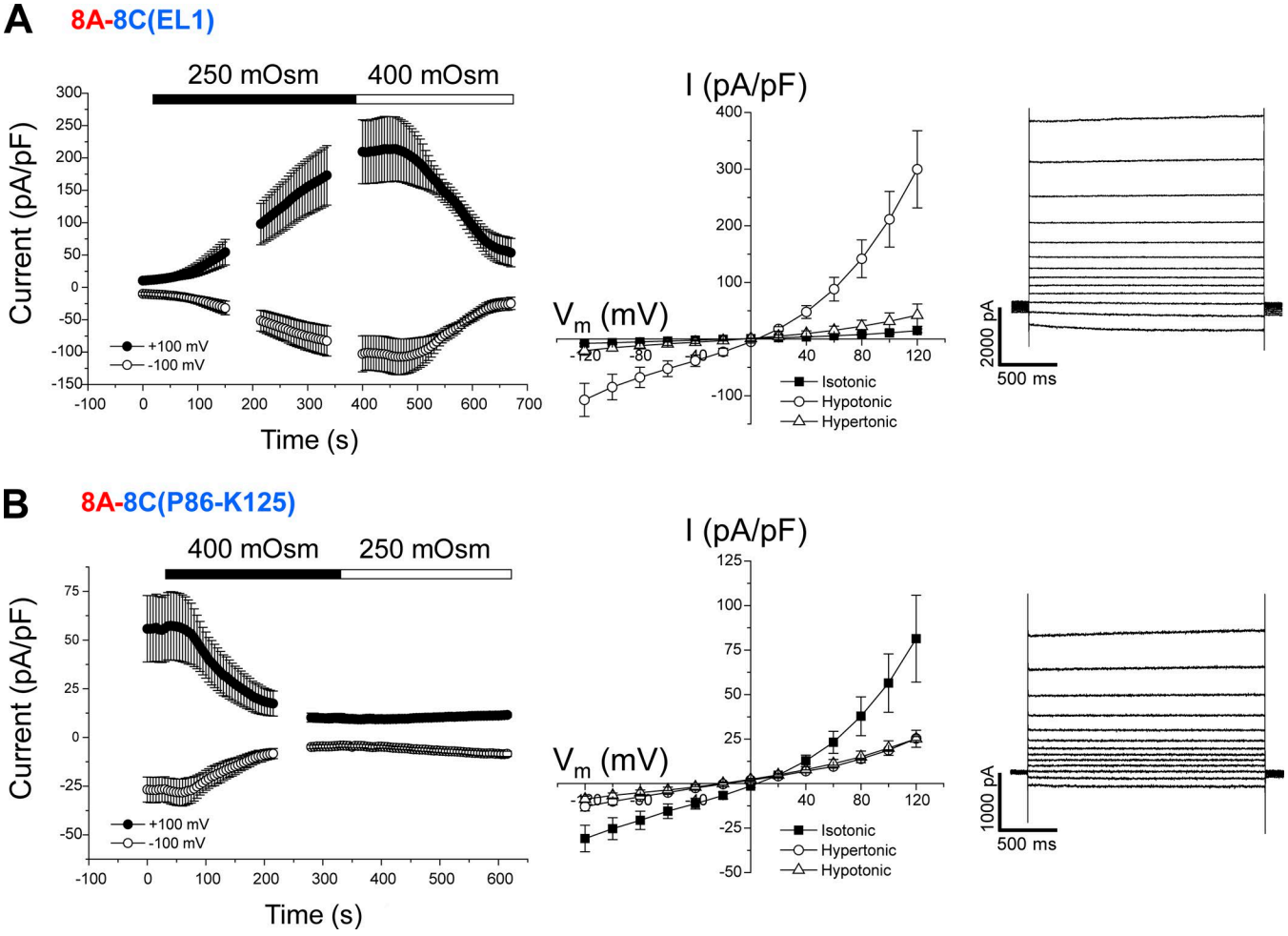

Figure 7. **Cell volume–sensitive currents induced by the homomeric 8A-8C(EL1) chimeras. (A)** Time course (left) and current–voltage relationships (middle) of resting, swelling-activated, and shrinkage-inactivated currents in *Lrrc8*$^{-/-}$ HCT116 cells expressing the 8A-8C(EL1) chimera. Values are means ± SEM (n = 5). Right panel shows representative traces of swelling-activated currents induced by the chimera. **(B)** Time course (left) and current–voltage relationships (middle) of resting and shrinkage-inactivated currents and currents observed in hypotonic medium in *Lrrc8*$^{-/-}$ HCT116 cells expressing the 8A-8C(P86–K125) chimera. Values are means ± SEM (n = 5). Right panel shows representative traces of currents induced by the chimera in isotonic medium.

adrenoreceptor (Billaud et al., 2015). Although speculative, it is interesting to postulate that D182–E206 of the LRRC8A IL may function as a MoRE/MoRF. This region could play a role in the assembly of LRRC8 subunits into VRACs and/or in VRAC regulation by cell volume changes. Extensive additional studies are required to test these hypotheses.

We observed significant changes in voltage sensitivity, anion permeability, and rectification of the 8C-8A(IL), 8D-8A(IL), and 8E-8A(IL) chimeras compared with 8A + 8C, 8A + 8D, and 8A + 8E heteromers (Table 1). However, interpretation of these results is not straightforward. It is unclear if heteromeric VRACs have a constant ratio of subunits and whether the subunits are assembled in a fixed order. Biochemical and functional data suggest that the subunit stoichiometries of VRAC heteromers may vary (Gaitán-Peñas et al., 2016; Lutter et al., 2017). If subunit stoichiometry and assembly affect channel properties, the properties of whole-cell VRAC currents would represent an ensemble average of all active channel types expressed in the cell membrane.

In contrast to VRAC heteromers, swelling-activated currents observed in cells expressing homomeric chimeras represent a single channel type. As shown in Fig. 6 and Table 2, LRRC8C and LRRC8E chimeras containing portions of the LRRC8A IL exhibit marked changes in anion permeability, rectification, and voltage sensitivity. These changes in channel electrophysiological properties suggest that the LRRC8A IL may play a role in VRAC pore structure and/or gating. Consistent with this idea, the IL of connexin 43 interacts with the cytoplasmic C terminus of the protein and plays a role in regulating voltage-dependent fast gating (Ponsaerts et al., 2012). Cryo-EM analysis of the structure of the innexin-6 gap junction indicates that the IL and C terminus interact to form a dome-like structure that may regulate pore conformation (Oshima et al., 2016).

The EL1s of connexins (Maeda et al., 2009) and pannexins (Wang and Dahl, 2010) are thought to contribute to pore structure. The LRRC8 EL1 has also been implicated in VRAC pore structure/function. Ullrich et al. (2016) recently demonstrated that charge reversal mutations in lysine and aspartate residues in the C-terminal portion of the EL1s of LRRC8A, LRRC8C, and LRRC8E altered VRAC iodide permeability and voltage-dependent gating.

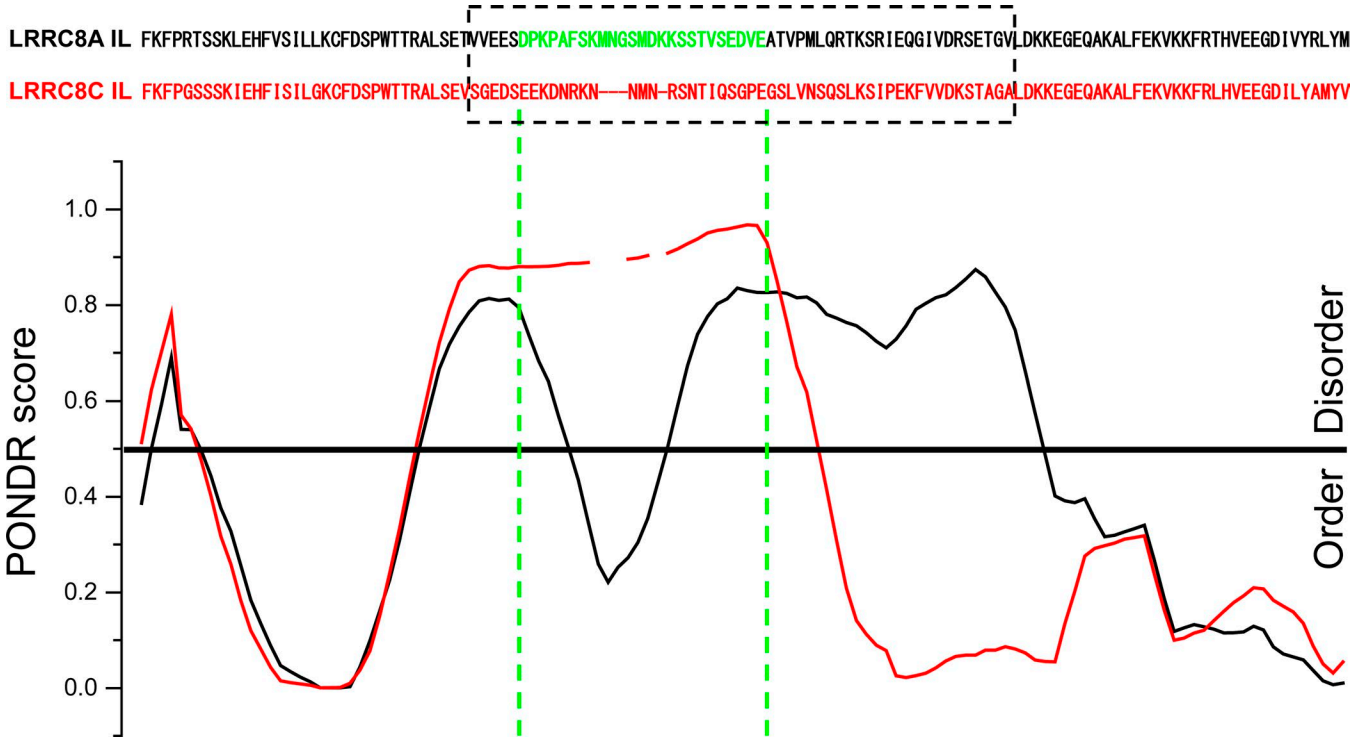

Figure 8. **PONDR VLXT analysis of LRRC8A (black) and LRRC8C (red) ILs.** PONDR scores are aligned with specific amino acid residues, which are shown at the top. The dashed box shows amino acid sequences that diverge significantly in LRRC8A, LRRC8C, LRRC8D, and LRRC8E proteins (Fig. 2). Amino acids colored green (D182–E206) in the LRRC8A sequence are the minimal sequence required to give rise to chimeric homomeric 8C-8A(IL) and 8E-8A(IL) VRACs with normal swelling-induced activity.

Using a chimera approach, Ullrich et al. (2016) also showed that the last 33 amino acids of EL1 of LRRC8C and LRRC8E were critical for determining the characteristics of voltage-dependent inactivation. LRRC8A + LRRC8C heteromers show weak inactivation at positive membrane voltages (Fig. 1 D), whereas LRRC8A + LRRC8E are strongly inactivated (Figs. 5 A). Swapping the last 33 amino acids of EL1 in LRRC8C with those of LRRC8E is sufficient to induce LRRC8E-like voltage-dependent properties in LRRC8A + LRRC8C heteromers and vice versa.

We were unable to identify specific regions of EL1 essential for homomeric VRAC function. Four partial 8A-8C(EL1) chimeras we engineered failed to give rise to normal VRAC activity (unpublished data). Interestingly, a partial 8A-8C chimera containing the last 39 amino acids of the LRRC8C EL1 (8A-8C[P86–K125]) gave rise to large constitutively active anion currents that were inactivated by cell shrinkage but insensitive to cell swelling (Fig. 7 B). Additional studies are required to determine the precise structure/function roles of EL1. The ability to dissociate sensitivity from cell swelling and shrinkage in this chimera may also provide unique insights into how VRAC detects cell volume changes.

In conclusion, we have demonstrated for the first time that homomeric VRAC channels can be generated by chimeric LRRC8 proteins. Normal VRAC activity is observed in LRRC8C, LRRC8D, and LRRC8E chimeras in which their intracellular loops are replaced by the LRRC8A IL. Insertion of a 25–amino acid sequence of the LRRC8A IL into either LRRC8C or LRRC8E gives rise to normal VRAC channels. Finally, replacing EL1 of LRRC8A with the LRRC8C EL1 also generates normal VRAC activity. Our results, as well as the findings of others (Ullrich et al., 2016), suggest that EL1 and the LRRC8A IL may play important roles in VRAC pore structure/function. Both loops may also play roles in VRAC assembly and volume-dependent regulation. Homomeric LRRC8 channels will greatly simplify future studies aimed at understanding channel structure/function relationships and the longstanding and vexing problem of how VRAC is regulated by cell volume changes.

Acknowledgments

We thank Cammie Phalan and Becky Morrison for technical assistance.

This work was supported by National Institute of Diabetes and Digestive and Kidney Diseases grant R01 DK51610 to K. Strange and by National Institute of General Medical Sciences Institutional Development Award grant P20 GM103423 and Center of Biomedical Research Excellence grant P20 GM104318.

The authors declare no competing financial interests.

Author contributions: T. Yamada and K. Strange proposed and designed the studies described in this paper. T. Yamada performed the experimental studies. T. Yamada and K. Strange participated in the analysis and interpretation of the data, in the writing of the manuscript, and in the approval of the final version of the manuscript for publication.

Merritt C. Maduke served as editor.

Note added in proof. After acceptance of this manuscript for publication, Deneka et al. (Deneka et al. 2018. *Nature*. https://doi

.org/10.1038/s41586-018-0134-y) defined the cryo-EM structures of a homomeric LRRC8A channel and a heteromeric LRRC8A + LRRC8C channel. Both channels are hexamers.

Submitted: 30 January 2018
Revised: 2 April 2018
Accepted: 1 May 2018

References

Abascal, F., and R. Zardoya. 2012. LRRC8 proteins share a common ancestor with pannexins, and may form hexameric channels involved in cell-cell communication. *BioEssays.* 34:551–560. https://doi.org/10.1002/bies.201100173

Ambrosi, C., O. Gassmann, J.N. Pranskevich, D. Boassa, A. Smock, J. Wang, G. Dahl, C. Steinem, and G.E. Sosinsky. 2010. Pannexin1 and Pannexin2 channels show quaternary similarities to connexons and different oligomerization numbers from each other. *J. Biol. Chem.* 285:24420–24431. https://doi.org/10.1074/jbc.M110.115444

Billaud, M., Y.H. Chiu, A.W. Lohman, T. Parpaite, J.T. Butcher, S.M. Mutchler, L.J. DeLalio, M.V. Artamonov, J.K. Sandilos, A.K. Best, et al. 2015. A molecular signature in the pannexin1 intracellular loop confers channel activation by the α1 adrenoreceptor in smooth muscle cells. *Sci. Signal.* 8:ra17. https://doi.org/10.1126/scisignal.2005824

Bond, S.R., and C.C. Naus. 2012. RF-Cloning.org: An online tool for the design of restriction-free cloning projects. *Nucleic Acids Res.* 40(W1):W209–W213. https://doi.org/10.1093/nar/gks396

Chiu, Y.H., M.S. Schappe, B.N. Desai, and D.A. Bayliss. 2018. Revisiting multimodal activation and channel properties of Pannexin 1. *J. Gen. Physiol.* 150:19–39. https://doi.org/10.1085/jgp.201711888

Gaitán-Peñas, H., A. Gradogna, L. Laparra-Cuervo, C. Solsona, V. Fernández-Dueñas, A. Barrallo-Gimeno, F. Ciruela, M. Lakadamyali, M. Pusch, and R. Estévez. 2016. Investigation of LRRC8-mediated volume-regulated anion currents in *Xenopus* oocytes. *Biophys. J.* 111:1429–1443. https://doi.org/10.1016/j.bpj.2016.08.030

Gradogna, A., P. Gavazzo, A. Boccaccio, and M. Pusch. 2017. Subunit-dependent oxidative stress sensitivity of LRRC8 volume-regulated anion channels. *J. Physiol.* 595:6719–6733. https://doi.org/10.1113/JP274795

Hoffmann, E.K., I.H. Lambert, and S.F. Pedersen. 2009. Physiology of cell volume regulation in vertebrates. *Physiol. Rev.* 89:193–277. https://doi.org/10.1152/physrev.00037.2007

Hyzinski-García, M.C., A. Rudkouskaya, and A.A. Mongin. 2014. LRRC8A protein is indispensable for swelling-activated and ATP-induced release of excitatory amino acids in rat astrocytes. *J. Physiol.* 592:4855–4862. https://doi.org/10.1113/jphysiol.2014.278887

Jentsch, T.J. 2016. VRACs and other ion channels and transporters in the regulation of cell volume and beyond. *Nat. Rev. Mol. Cell Biol.* 17:293–307. https://doi.org/10.1038/nrm.2016.29

Lutter, D., F. Ullrich, J.C. Lueck, S. Kempa, and T.J. Jentsch. 2017. Selective transport of neurotransmitters and modulators by distinct volume-regulated LRRC8 anion channels. *J. Cell Sci.* 130:1122–1133.

Ma, Z., J.E. Tanis, A. Taruno, and J.K. Foskett. 2016. Calcium homeostasis modulator (CALHM) ion channels. *Pflugers Arch.* 468:395–403. https://doi.org/10.1007/s00424-015-1757-6

Maeda, S., S. Nakagawa, M. Suga, E. Yamashita, A. Oshima, Y. Fujiyoshi, and T. Tsukihara. 2009. Structure of the connexin 26 gap junction channel at 3.5 A resolution. *Nature.* 458:597–602. https://doi.org/10.1038/nature07869

Mohan, A., C.J. Oldfield, P. Radivojac, V. Vacic, M.S. Cortese, A.K. Dunker, and V.N. Uversky. 2006. Analysis of molecular recognition features (MoRFs). *J. Mol. Biol.* 362:1043–1059. https://doi.org/10.1016/j.jmb.2006.07.087

Nilius, B., and G. Droogmans. 2003. Amazing chloride channels: An overview. *Acta Physiol. Scand.* 177:119–147. https://doi.org/10.1046/j.1365-201X.2003.01060.x

Oldfield, C.J., Y. Cheng, M.S. Cortese, P. Romero, V.N. Uversky, and A.K. Dunker. 2005. Coupled folding and binding with alpha-helix-forming molecular recognition elements. *Biochemistry.* 44:12454–12470. https://doi.org/10.1021/bi050736e

Oshima, A., K. Tani, and Y. Fujiyoshi. 2016. Atomic structure of the innexin-6 gap junction channel determined by cryo-EM. *Nat. Commun.* 7:13681. https://doi.org/10.1038/ncomms13681

Phelan, P. 2005. Innexins: Members of an evolutionarily conserved family of gap-junction proteins. *Biochim. Biophys. Acta.* 1711:225–245. https://doi.org/10.1016/j.bbamem.2004.10.004

Planells-Cases, R., D. Lutter, C. Guyader, N.M. Gerhards, F. Ullrich, D.A. Elger, A. Kucukosmanoglu, G. Xu, F.K. Voss, S.M. Reincke, et al. 2015. Subunit composition of VRAC channels determines substrate specificity and cellular resistance to Pt-based anti-cancer drugs. *EMBO J.* 34:2993–3008. https://doi.org/10.15252/embj.201592409

Ponsaerts, R., N. Wang, B. Himpens, L. Leybaert, and G. Bultynck. 2012. The contractile system as a negative regulator of the connexin 43 hemichannel. *Biol. Cell.* 104:367–377. https://doi.org/10.1111/boc.201100079

Qiu, Z., A.E. Dubin, J. Mathur, B. Tu, K. Reddy, L.J. Miraglia, J. Reinhardt, A.P. Orth, and A. Patapoutian. 2014. SWELL1, a plasma membrane protein, is an essential component of volume-regulated anion channel. *Cell.* 157:447–458. https://doi.org/10.1016/j.cell.2014.03.024

Schober, A.L., C.S. Wilson, and A.A. Mongin. 2017. Molecular composition and heterogeneity of the LRRC8-containing swelling-activated osmolyte channels in primary rat astrocytes. *J. Physiol.* 595:6939–6951. https://doi.org/10.1113/JP275053

Strange, K. 1998. Molecular identity of the outwardly rectifying, swelling-activated anion channel: Time to reevaluate pICln. *J. Gen. Physiol.* 111:617–622. https://doi.org/10.1085/jgp.111.5.617

Syeda, R., Z. Qiu, A.E. Dubin, S.E. Murthy, M.N. Florendo, D.E. Mason, J. Mathur, S.M. Cahalan, E.C. Peters, M. Montal, and A. Patapoutian. 2016. LRRC8 proteins form volume-regulated anion channels that sense ionic strength. *Cell.* 164:499–511. https://doi.org/10.1016/j.cell.2015.12.031

Ullrich, F., S.M. Reincke, F.K. Voss, T. Stauber, and T.J. Jentsch. 2016. Inactivation and anion selectivity of volume-regulated anion channels (VRACs) depend on C-terminal residues of the first extracellular loop. *J. Biol. Chem.* 291:17040–17048. https://doi.org/10.1074/jbc.M116.739342

Venkatesh, B., A.P. Lee, V. Ravi, A.K. Maurya, M.M. Lian, J.B. Swann, Y. Ohta, M.F. Flajnik, Y. Sutoh, M. Kasahara, et al. 2014. Elephant shark genome provides unique insights into gnathostome evolution. *Nature.* 505:174–179. https://doi.org/10.1038/nature12826

Voss, F.K., F. Ullrich, J. Münch, K. Lazarow, D. Lutter, N. Mah, M.A. Andrade-Navarro, J.P. von Kries, T. Stauber, and T.J. Jentsch. 2014. Identification of LRRC8 heteromers as an essential component of the volume-regulated anion channel VRAC. *Science.* 344:634–638. https://doi.org/10.1126/science.1252826

Wang, J., and G. Dahl. 2010. SCAM analysis of Panx1 suggests a peculiar pore structure. *J. Gen. Physiol.* 136:515–527. https://doi.org/10.1085/jgp.201010440

Wine, J.J., and D.B. Luckie. 1996. Cell-volume regulation: P-glycoprotein–a cautionary tale. *Curr. Biol.* 6:1410–1412. https://doi.org/10.1016/S0960-9822(96)00744-0

Xue, B., A.K. Dunker, and V.N. Uversky. 2010. Retro-MoRFs: Identifying protein binding sites by normal and reverse alignment and intrinsic disorder prediction. *Int. J. Mol. Sci.* 11:3725–3747. https://doi.org/10.3390/ijms11103725

Yamada, T., R. Wondergem, R. Morrison, V.P. Yin, and K. Strange. 2016. Leucine-rich repeat containing protein LRRC8A is essential for swelling-activated Cl^- currents and embryonic development in zebrafish. *Physiol. Rep.* 4:e12940. https://doi.org/10.14814/phy2.12940

Zou, J., M. Salarian, Y. Chen, R. Veenstra, C.F. Louis, and J.J. Yang. 2014. Gap junction regulation by calmodulin. *FEBS Lett.* 588:1430–1438. https://doi.org/10.1016/j.febslet.2014.01.003